



# Potential Applications of Multiband Spectroscopy and Hyperspectral Imaging for Detecting HLB Infected Orange Trees

ASHISH MISHRA, REZA EHSANI\*, DAVOOD KARIMI, AND L. GENE ALBRIGO

University of Florida, IFAS, Citrus Research and Education Center, Lake Alfred, FL 33850

**ADDITIONAL INDEX WORDS.** *Diaphorina citri*, Huanglongbing (HLB), hyperspectral, spectroscopy, logistic regression, weighted k-nearest neighbors, support vector machine

**Huanglongbing (HLB) or citrus greening is a bacterial disease threatening Florida's multi-billion dollar citrus industry. Currently, the best management practice to control the disease is to detect the infected tree and remove it as soon as possible as the infected tree can be the inoculum source resulting in further spread of the disease. Scouting and visual inspection for the disease symptoms is currently used by growers to identify HLB-infected trees. However, this method is very time consuming, subjective, and expensive. Therefore, the long-term goal of this research is to develop a fast screening technique that can assist citrus growers in detecting HLB-infected citrus trees. In this study, a rugged, low-cost, multi-band active optical sensor and hyperspectral imaging were used to identify HLB-infected trees from healthy trees. Analysis of the multi-band optical sensor data showed that due to the large variability in the data, it was not possible to discriminate the healthy trees from that of infected trees based only on a single measurement from a tree. However, using multiple measurements from a tree, it was possible to achieve high classification accuracy. With three measurements, k-nearest neighbors and support vector machines yielded classification errors of less than 5%. Normalized Difference Vegetation Index (NDVI), Simple Ratio Index (SR), Modified Triangular Vegetation Index (MTVI-2), Renormalized Difference Vegetation Index (RDVI) and Structure Intensive Pigment Index (SIPI) are indices that were evaluated for healthy and HLB infected trees based on the optical sensor and hyperspectral imaging results. These vegetative indices showed potential to differentiate HLB trees from healthy trees with multi band optical sensor as well as hyperspectral camera. The results demonstrate the potential of a multi-band active optical sensor and hyperspectral camera for detecting HLB-infected citrus trees under field conditions.**

Florida accounts for 70% of total US citrus production and produced 7236 tons of citrus from 224,358 ha (554,400 acres) of bearing orchards in 2006–07 (FASS, 2008). Huanglongbing (HLB), also known as greening is a systemic bacterial disease transmitted by the Asian citrus (*Diaphorina citri*) psyllid insect. This disease is considered as one of the most devastating citrus diseases in the world. HLB was first detected in Florida in Aug. 2005 (Manjunath, 2008). As HLB is a relatively new disease in the US, very little published information is available on its dynamics and epidemiology under Florida conditions. HLB symptoms in leaves include blotchy mottle, leatheriness, vein clearing, and vein yellowing or corking. The blotchy mottle is specific to the HLB disease and consists of blotches of yellow on dark greenish-gray leaves (Fig. 1). The healthy citrus leaves are presented in Fig. 2.

Currently, the detection of HLB relies on scouting orchards for visible symptoms and following up with off-site diagnosis of the disease using a polymerase chain reaction technique. Once the presence of HLB trees are confirmed, the suspected tree is removed, and control of the vector Asian citrus psyllid is imple-

mented. Scouting is laborious, time consuming, often subjective, and prone to errors. Knowledgeable growers in Brazil estimate that at least 50% of infected trees with visible symptoms go undetected by trained scouts, even while using an observation platform. Similar results have been reported in Florida (Futch et al., 2009).

Reflectance spectra of vegetation measured in the visible and infrared regions contain information on plant pigment concentration, leaf cellular structure, and leaf moisture content (Borengasser et al., 2001). Carter and Knapp (2001) reported good linear



Fig. 1. HLB infected leaves.

**Acknowledgments.** This project was supported by a grant from the Florida Citrus Production Research Advisory Council. Authors would like to thank Sherry Buchanan at the Citrus Research and Education Center, Lake Alfred, FL, for her help in data collection. We would also like to extend our thanks to the crews of Lykes Bros. Inc., Lake Placid, FL, SWFREC at Immokalee and Southern Gardens Citrus near Clewiston for their assistance in this project.

\*Corresponding author; email: Ehsani@crec.ifas.ufl.edu; phone: (863) 956-1151, ext. 1228



Fig. 2. Healthy leaves.

relationship between leaf chlorophyll and spectral reflectance in sweet gum, red maple, wild grape, switch cane, and longleaf pine. Such band-specific information on reflectance can help in discriminating HLB infected trees in the citrus grove.

Rapid, early, and accurate diagnosis, especially at the orchard level, is essential to contain and eliminate the disease threat at the primary stages of infection. The present work focuses on imaging and spectral techniques for rapid detection of diseases to prevent the development and spread of the citrus disease. The specific objectives of this study were:

- To develop and evaluate a multi-band active optical sensor for detecting HLB infected citrus trees under field conditions.
- To assess hyperspectral imaging technique for HLB detection under field conditions.

### Material and Methods

**DEVELOPMENT OF THE FOUR-BAND OPTICAL SENSOR.** A preliminary study was conducted to select the spectral bands representative of HLB disease in citrus trees. In the preliminary analysis, the reflectance measurements from the citrus canopy were collected using FieldSpec® 3 spectroradiometer [Analytical Spectral Device (ASD), Boulder, CO]. The reflectance data were acquired from 350 to 2500 nm wavelength.

The reflectance data were analyzed and it was found that four wavelengths (570, 670, 870, and 970 nm) provided the maximum classification accuracy for differentiating HLB infected trees from healthy trees. These four bands were selected for developing a multi-band active optical sensor (Mishra et al., 2007). The sensor was developed by Applied Technology (Stillwater, OK). The sensor was composed of four narrow-band (active optic) light sources with four different wavelengths: two in the visible region (at 570 and 670 nm) and two in the near infrared region (at 870 and 970 nm). After lighting the target, the light was reflected and captured by a receiver located in the center of the device. The sensor automatically acquired the values of reflectance for each of the four wavelengths. The sensor was interfaced with a hand-held PDA through a serial port. This sensor does not need reference because it works on relative values not on the absolute values. The reflectance data and the internal temperature of the unit at the time of reading were recorded and saved in the PDA. Figure 3 depicts the optical sensor used in this study.

**FIELD EXPERIMENTS USING THE FOUR-BAND OPTICAL SENSOR.** The spectral data with the four band sensor were collected in a grove near Fort Basinger, FL with the 'Mid-sweet' orange variety. Three HLB-infected trees and three healthy trees (close to HLB-infected trees) were used in this experiment. Ten readings of HLB symptomatic and non-symptomatic leaves from HLB-infected trees as well as 10 readings from the healthy tree leaves were collected. The average of these 10 readings is the representative value of reflectance of the HLB symptomatic, HLB non-symptomatic, and healthy trees. Measurements of reflectance were made at a distance of about 1 m between the sensor and the target (Fig. 4). In our preliminary test we found our sensor works well below 1000 lux. The experimental conditions were standardized based on some preliminary tests. The data were collected on 27 Aug. and 17 Sept. 2008.

**FIELD EXPERIMENTS FOR HYPERSPECTRAL IMAGING.** Hyperspectral images were collected with a hyperspectral camera



Fig. 3. Multi-band active optical sensor.



Fig. 4. Data collection with multi-band active optical sensor.

(Autovision, Los Angeles, CA) having a spectral range from 306.5 to 1067.1 nm with 2.7 nm spectral resolution. The camera consists of 135 bands. Images were collected from the grove at Fort Basinger, Southwest Florida Research and Education Center (SWFREC) at Immokalee, and a grove near Clewiston, FL. A total of 10 images (5 HLB, 5 Healthy) in the first two locations and 20 images (13 HLB, 7 Healthy) at the third location were evaluated in this study. All the field data were collected during 10:00 AM to 2:00 PM. Reference reading for white panel was also collected at the same time. Therefore, there is negligible effect of ambient light in the data collection.

### Data Analysis

**FOUR-BAND OPTICAL SENSOR.** For the experiments using the optical sensor, each measurement was composed of the four reflectance values at 570, 670, 870, and 970 nm. Using these values, 11 different vegetative indices were computed. Table 1 shows the details of vegetative indices used in the study.

Outliers in the data were first detected and removed. This was done by performing a principal component analysis on the data and plotting the first four principal components. From this analysis, 20 of the 1552 measurements were recognized as outliers and removed. Three different classification techniques were applied to classify the HLB-infected trees from the healthy trees based on the four band optical sensor data. The detailed description of these methods is described in Mishra et al. (2009). In the following paragraphs, these techniques are briefly described.

Table 1. List of vegetative indices used in analysis.

Vegetative Index (VI)	Equation
Normalized Difference Vegetation Index (NDVI-1), Rouse <i>et al.</i> (1974)	$NDVI - 870 = \frac{R_{870} - R_{670}}{R_{870} + R_{670}}$
NDVI-2	$NDVI - 970 = \frac{R_{970} - R_{670}}{R_{970} + R_{670}}$
Simple Ratio Index (SR-1), Rouse <i>et al.</i> (1974)	$SR - 870 = \frac{R_{870}}{R_{670}}$
Simple Ratio Index (SR-2)	$SR - 970 = \frac{R_{970}}{R_{670}}$
Modified Triangular Vegetation Index (MTVI-1), Haboudane <i>et al.</i> (2004)	$TVI - 1 = 1.2[1.2(R_{870} - R_{570}) - 2.5 \times (R_{670} - R_{570})]$
Modified Triangular Vegetation Index (MTVI-2), Haboudane <i>et al.</i> (2004)	$MTVI - 2 = \frac{1.5[1.2 \times (R_{870} - R_{570}) - 2.5 \times (R_{670} - R_{570})]}{\sqrt{(2 \times R_{870} + 1)^2 - (6 \times R_{870} - 5 \times \sqrt{R_{670}}) - 0.5}}$
Renormalized Difference Vegetation Index (RDVI), Rougean and Breon (1995),	$RDVI = \frac{(R_{870} - R_{670})}{\sqrt{(R_{870} + R_{670})}}$
Greenness Index (G)	$G = \frac{R_{550}}{R_{670}}$
Triangular Veg. Index (TVI), Broge and Leblanc (2000)	$TVI = 0.5 \times [120 \times (R_{870} - R_{570}) - 200 \times (R_{670} - R_{570})]$
Modified Chlorophyll Absorption in Reflectance Index (MCARI), Daughtry <i>et al.</i> (2000)	$MCARI = 1.2 \times [(2.5 \times R_{870} - R_{670}) - 1.3 \times (R_{870} - R_{570})]$
Structure Intensive Pigment Index (SIP), Penuelas <i>et al.</i> (1995)	$SIP = (R_{870} - R_{570}) / (R_{870} + R_{670})$

**1. K-NEAREST NEIGHBORS (KNN).** A weighed k-nearest neighbor scheme was used with weights inversely proportional to the square of Euclidian distance (Fukunaga, 1990).

**2. LOGISTIC REGRESSION.** In this method, the goal was to adjust the parameters ( $\theta$ ) of the logistic curve in order to best fit the curve to the training data (Larose, 2006).

$$f_{\theta}(x) = \frac{1}{1 + e^{-\theta^T x}} \quad (\text{Eq. 1})$$

A batch gradient descent method was used to find the optimum values for the parameters  $\theta$ .

**3. SUPPORT VECTOR MACHINES (SVM).** This technique involves finding the hyperplane, which separates the data with the largest possible margin. In this study, a modified SVM method (Webb, 2002) with a Gaussian kernel was used. Optimization problem was performed using:

$$\max_{\alpha} \sum_{i=1}^N \alpha_i - \frac{1}{2} \sum_{i,j=1}^N y^i y^j \alpha_i \alpha_j K(x^i, x^j)$$

such that:  $C \geq \alpha_i \geq 0, i = 1, \dots, N$

$$\sum_{i=1}^N \alpha_i y^i = 0$$

$$\text{where: } K(x^i, x^j) = \exp(-\gamma \|x^i - x^j\|^2) \quad (\text{Eq. 2})$$

After optimization, the optimal margin classifier was formed as:

$$y = f\left(\sum_{i=1}^N \alpha_i y^i(x, x^i) + w_0\right) \quad (\text{Eq. 3})$$

where:

$$w = \sum_{i=1}^N \alpha_i y^i x^i$$

$$w_0 = -\frac{\max_{i,y^i=1} w^T x^i + \min_{i,y^i=-1} w^T x^i}{2} \quad (\text{Eq. 4})$$

In equation 3,  $f(t) = 1$  if  $t \geq 0$ , and  $f(t) = -1$  if  $t < 0$ , where labels “1” and “-1” represent the two classes that the classifier separates. In this study, we used the sequential minimal optimization (SMO) algorithm (Platt, 1998) to solve this problem.

**HYPERSPECTRAL IMAGING.** The hyperspectral images were analyzed using image processing technique. The hyperspectral images were imported in remote sensing software ENVI 4.5 (ITT Visual Information Solutions, Boulder, CO). Since noisy data was acquired between 306 and 420 nm, and bands after 870 nm, these bands were eliminated from the data and a total of 80 bands were used in the analysis. Dark subtraction was applied by minimum pixel value to remove background information (sky, grass, soil, etc.). Images were calibrated by the flat field method (Fig. 5a). Masks were created to filter other objects except the tree (Fig. 5b). Images with only tree (region of interest) were obtained by applying these masks (Fig. 5c) Average pixel values were computed for each band. Various vegetative indices were computed as given in Table 1.

## Results and Discussion

**FOUR-BAND OPTICAL SENSOR.** The four-band optical sensor data was classified using the three classification models. Table 2 summarizes the results obtained from the three classification methods



Fig.5a. Raw image acquired from hyperspectral camera.

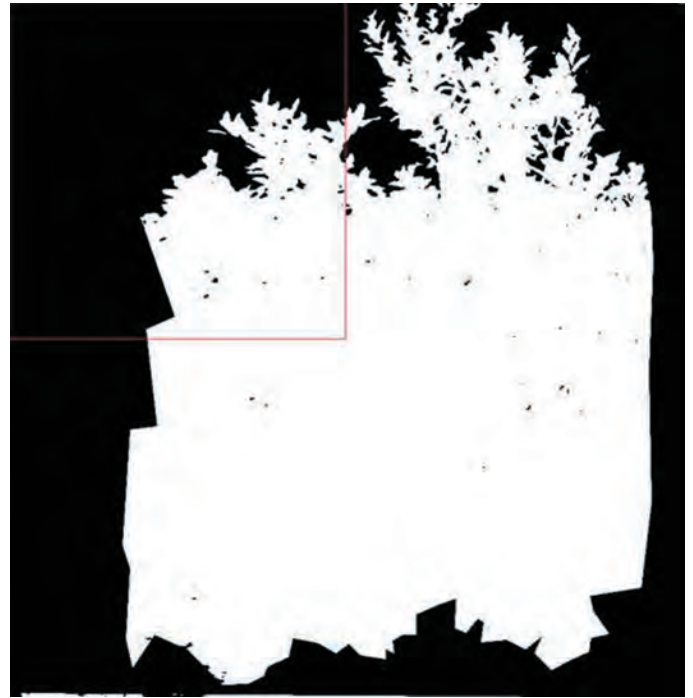


Fig.5b. Preprocessed image after masking (Background as sky, soil, grass removed).

used in this study. As seen from Table 2, the classification error for each of the classification methods was higher when only one measurement from the tree was tested. The classification error from the classification models was >17%. Because the classification errors were high, it was decided to evaluate the performance of the classifiers with more than one measurement as an input in the testing phase. When three and five measurements from the same tree were used to classify the data, it was found that the classification error decreased (Table 2). With five measurements, the k-nearest neighbors and support vector machine resulted in <5% error. The criteria for classification was that if the classifier labeled more than half of the measurements as “HLB-infected,” then the final prediction was also “HLB-infected,” or else the final prediction was “healthy.” The classification error reduced significantly with multiple measurements. The possible reason for high classification error with single measurements was due to the large variability in the field measurements, which might have resulted from environmental factors (such as the orientation of the leaves with respect to the sensor, wind) and operator error (such as the non-constant distance between the sensor and the leaves). Using multiple measurements reduced these sources of noise and allowed higher classification accuracies. SVM and KNN achieved an accuracy of higher than 95% with five measurements from each tree.

**HYPER SPECTRAL IMAGING.** Statistical analysis was performed to see the difference between vegetative indices of HLB-infected tree and healthy trees. In this analysis we used completely randomized design. We collected hyperspectral images of HLB infected tree and healthy tree. Our null hypothesis was  $H_0: \mu_{HLB} = \mu_{Healthy}$ .

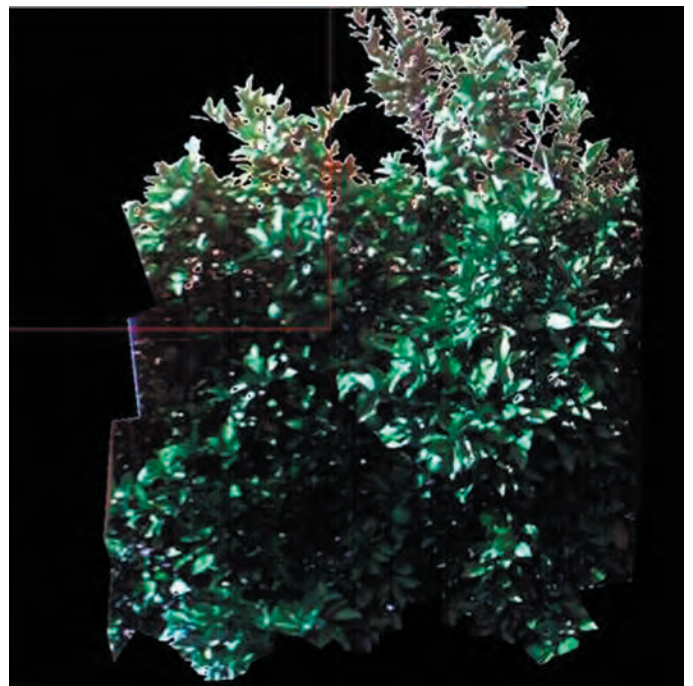


Fig. 5c. Processed image used for data analysis.

Table 2. Average classification error for different classification techniques.

Statistical methods	Logistic regression	k-nearest neighbors	Support vector machines
Error with one set of measurements (%)	40	18	17
Error with three sets of measurements (%)	35	8.5	7.5
Error with five sets of measurements (%)	32	4.5	3.5

Table 3. Means of vegetative indices of HLB-infected and healthy trees showing statistically significant difference at  $\alpha = 0.05$

Vegetative indices	HLB	Healthy
Normalized Difference Vegetation Index (NDVI <sub>870</sub> )	0.49	0.72
Simple Ratio Index (SR <sub>870</sub> )	3.96	6.80
Modified Triangular Vegetation Index (MTVI <sub>2</sub> )	0.50	0.72
Renormalized Difference Vegetation Index (RDVI)	0.45	0.63
Structure Intensive Pigment Index (SIPI)	0.34	0.58

We ran ANOVA to see if our hypothesis was accepted or rejected at  $\alpha = 0.05$ . Table 3 shows only those vegetative indices which means were significant different based on *P* value.

Among the estimated vegetative indices (Table 1), few vegetative indices (Table 3) were found to be statistically significant to differentiate between HLB-infected trees and healthy trees. For example, Normalized Difference Vegetation Indices (NDVI<sub>870</sub>) for HLB-infected trees and healthy trees were 0.49 and 0.79, respectively. Similarly, other vegetative indices that show significant difference between HLB infected trees and healthy trees are described in Table 3. The results exhibited a potential for using hyperspectral imaging to detect HLB infected trees from that of healthy trees.

### Conclusions

The results show that the four-band sensor developed in this study has a very good potential for detecting HLB-infected citrus trees in the field. To obtain high classification accuracy, however, it is necessary to acquire multiple measurements from a single tree. The sensor also has the potential for being integrated into the scouting practice. Obtaining multiple readings using this sensor is easy and fast, and can be done by a human or an automated system. Hyperspectral imaging also demonstrated good potential to discriminate HLB-infected and healthy trees. Future studies involve the evaluation of the imaging and optical sensor for discriminating nutrient deficient tree and trees infected with other diseases. The measurements in this study were performed on one cultivar of orange. It will be necessary to assess the sensor and the classification algorithms for their performance with respect to other orange cultivars and citrus trees.

### Literature Cited

- Borengasser, M., T.R. Gottwald, and T. Riley. 2001. Spectral reflectance of citrus canker. *Proc. Fla. State Hort. Soc.* 114:77–79.
- Broge, N.H. and E. Leblanc. 2000. Comparing prediction power and stability of broadband and hyperspectral vegetation indices for estimation of green leaf area index and canopy chlorophyll density. *Remote Sens. Environ.* 76:156–172.
- Carter, G.A. and A.K. Knapp. 2001. Leaf optical properties in higher plants: Linking spectral characteristics stress and chlorophyll concentration. *Amer. J. Bot.* 88(4):677–684.
- Daughtry, C.S.T., C.L. Walthall, L. Kim, M.S. Kim, E. Brown de Colestoun, and J.E. McMurtrey III. 2000. Estimating corn leaf chlorophyll concentration from leaf and canopy reflectance. *Remote Sens. Environ.* 74:229–239.
- Florida Agriculture Statistics Services (FASS). 2008. Florida annual statistical bulletin. Available at: <[http://www.nass.usda.gov/Statistics\\_by\\_State/Florida/](http://www.nass.usda.gov/Statistics_by_State/Florida/)>.
- Fukunaga, K. 1990. Introduction to statistical pattern recognition, 2nd ed. Academic Press, San Diego, CA.
- Futch, S., S. Weingarten, and M. Irely. 2009. Determining HLB infection levels using multiple survey methods in Florida citrus. *Proc. Fla. State Hort. Soc.* 122:152–157.
- Haboudane, D., J.R. Miller, E. Pattey, P.J. Zarco-Tejada, and I.B. Strachan. 2004. Hyperspectral vegetation indices and novel algorithms for predicting green LAI of crop canopies: Modeling and validation in the context of precision agriculture. *Remote Sens. Environ.* 90:337–352.
- Larose, D.T. 2006. Data mining methods and models. Wiley, Hoboken, NJ.
- Mishra, A., R. Ehsani, G. Albrigo, and W.S. Lee. Spectral characteristics of citrus greening using hyperspectral data. *Amer. Soc. Agr. Biolog. Eng.*, Minneapolis, MN, 17–20 June 2007. Paper No. 073056.
- Mishra, A.R., D. Karimi, R. Ehsani, and W.S. Lee. 2009. Identification of citrus greening (HLB) infected citrus trees using spectroscopy and statistical classification. Submitted in *Trans. Amer. Soc. Agr. Biolog. Eng.* 2009.
- Manjunath K.L., S. Halbert, C. Ramadugu, S. Webb, and R.F. Lee. 2008. Detection of *Candidatus Liberibacter asiaticus* in *Diaphorina citri* and its importance in the management of citrus huanglongbing disease. *Phytopathology* 98:387–396.
- Penuelas, J., I. Filella, P. Lloret, F. Mufioz, and M. Vilajeliu. 1995. Reflectance assessment of mite effects on apple trees. *Intl. J. Remote Sens.* 16:2727–2733.
- Platt, J. 1998. Fast training of support vector machines using sequential minimal optimization, p. 41–65. In: B. Scholkopf, C. Burges, and A. Smola (eds.). *Advances in kernel methods—Support vector learning*, eds. MIT Press, Cambridge, MA.
- Rouse, J.W., R.H. Haas, J.A. Schell, D.W. Deering, and J.C. Harlan. 1974. Monitoring the vernal advancements and retrogradation of natural vegetation. NASA/GSFC, Greenbelt, MD.
- Rougean, J.L. and F.M. Breon. 1995. Estimating PAR absorbed by vegetation from bidirectional reflectance measurements. *Remote Sens. Environ.* 51:375–384.
- Webb, A.R. 2002. Statistical pattern recognition, 2nd ed. Wiley, Chichester, UK.